

**VISCOUS FLOW OF ILMENITE-BEARING CUMULATES DURING LUNAR MAGMA OCEAN SOLIDIFICATION: CONSEQUENCES FOR LUNAR EVOLUTION.** N. Dygert<sup>1</sup>, Y. Liang<sup>2</sup>, G. Hirth<sup>2</sup>, N. Zhang<sup>3</sup>, <sup>1</sup>Department of Earth and Planetary Sciences, University of Tennessee, Knoxville (ndygert1@utk.edu), <sup>2</sup>Department of Earth, Environmental and Planetary Sciences, Brown University, <sup>3</sup>Institution of Earth and Space Sciences, Peking University.

**Introduction:** Cumulate mantle overturn is thought to be a consequence of crystallization of the lunar magma ocean (LMO). In the model, dense ilmenite-bearing cumulates (IBC) that solidified from the last dregs of the of the crystallizing LMO flow into underlying low density early (mafic) magma ocean cumulates as viscous solids [1,2]. The overturn model has been invoked to explain the perogenesis of high-Ti basalts [1] and their spatial concentration on the lunar nearside [2,3]. Recent experimental work characterized the rheology of ilmenite, placing constraints on the viscosity of the IBC and an ilmenite-bearing lunar mantle [4,5]. However, scant attention has been paid to viscous flow of IBC during LMO solidification, which largely determines the dynamics of subsequent cumulate mantle overturn (or lack thereof) [2]. Here we evaluate the influence of magma ocean cumulate rheology on the distribution of IBC during and after LMO crystallization and its implications.

**LMO solidification model:** We assume a Moon forming giant impact produced a whole body LMO. Until it became saturated in plagioclase after ~80% crystallization, the LMO cooled rapidly. Assuming blackbody radiation from a convecting LMO suggests this first stage of crystallization occurred over a timescale of thousands of years. A second (much slower) stage of solidification started after saturation the of the LMO in buoyant plagioclase produced a flotation crust. This later stage of solidification (which eventually produced the IBC) would have taken ~10 to ~200Myr depending on influences of tidal heating and impact bombardment [6].

If the magma ocean fractionally crystallized [7], early mafic LMO cumulates would themselves be unstably density stratified owing to an upward increase in Fe content of the cumulate pile. This could lead to overturn of the mafic cumulates before complete LMO solidification [2,8]. The timescale for overturn of early cumulates can be estimated for a fluid with constant viscosity and linear density variation with depth,  $t = (4\pi^2\mu)/(\Delta\rho g d)$ , where  $d$  is the layer thickness,  $g$  is gravitational acceleration,  $\mu$  is viscosity and  $\Delta\rho$  is the density difference across the layer [9-12]. For  $\Delta\rho = 100\text{kg/m}^3$ ,  $d = 1280\text{ km}$ ,  $\mu = 10^{20}\text{ Pa}\cdot\text{s}$  we obtain an overturn timescale <1Myr. Olivine viscosity depends on Fe content [13] and would thus decrease toward the top of the cumulate pile such that this estimate may represent an upper bound. The analysis suggests the mafic cumulates overturned before complete crystallization of the LMO and precipitation of the IBC [2,8]. This initial overturn has important consequences; (1) decompression melt produced by overturn of early

mafic cumulates would come along with and increase the Mg# of the LMO liquid parental to the IBC, (2) the initial overturn would juxtapose early Mg-rich LMO cumulates against the IBC parental liquid, (3) the selenotherm would be temporarily inverted. The IBC parental liquid would remain buoyant throughout the initial overturn [7].

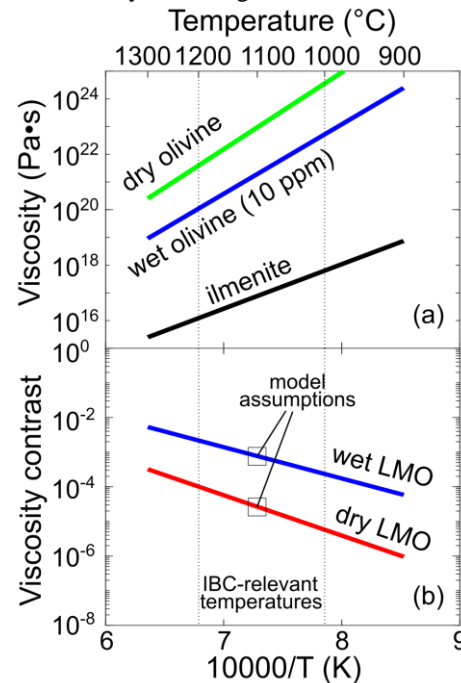


**Figure 1.** (a) Effective viscosity of wet and dry olivine [14] and ilmenite [4] in dislocation creep at a differential stress of 0.227MPa (consistent with the reference viscosity of [15]). In reality the stress may scale with the IBC layer thickness. (b) Viscosity contrast between ilmenite and dry olivine (red) and ilmenite and wet olivine (blue).

Fe-rich IBC have a crystallization temperature of ~1100-1000°C [10-12]; perhaps mixing of Mg-rich partial melts of overturned mafic cumulates increased the IBC crystallization temperature. We can assume the IBC did not precipitate until their parental liquid (the last dregs of the LMO) cooled below 1200°C [16]. This enables us to estimate the viscosity of the IBC and underlying cumulates; both likely deformed in dislocation creep (owing to the large grain sizes expected for cumulates of a magma ocean [17]). Taking the dislocation creep flow laws at face value, the viscosity contrast between the IBC and early LMO cumulates is largely determined by the LMO water content (Figs. 1a,b). The viscosity contrast is >4 orders of magnitude for a dry Moon; for a Moon with 10ppm H<sub>2</sub>O olivine it is >2 orders of magnitude. We

caution that recent experiments suggest Mg#40 ilmenite (in equilibrium with Mg#90 olivine) has a moderately higher viscosity than Fe end-member ilmenite.

**Viscous flow of IBC during LMO solidification:** Dense IBC would start sinking into overturned mafic cumulates as Rayleigh-Taylor (R-T) instabilities before complete LMO solidification. The timescale for formation of IBC R-T instabilities, instability wavelength, volume, and sinking rate depend on the viscosity contrast between the IBC and mafic cumulates (Fig. 1b) and the thickness of the IBC layer. The steady-state IBC layer thickness is determined by a competition between sedimentation of IBC from the crystallizing LMO and the growth of IBC instabilities [2]. The steady-state layer thickness ( $h$ ) can be approximated by equating the thickening rate of the IBC layer with the rate of diapir formation; [2] obtained the following expression,  $h \approx ((6.5\mu_{IBC}^{1/3}\mu_{MAFIC}^{2/3}s)/(\Delta\rho g))^{1/2}$ , where  $s$  is the solidification rate and  $\mu_{IBC}$  and  $\mu_{MAFIC}$  are the viscosities of the IBC and mafic cumulates respectively (Fig. 2a). Using this steady state layer thickness and the viscosities implied by the pure phase flow laws at 1100°C we calculate the wavelength of the R-T instabilities ( $\lambda = 2.9h(\mu_{MAFIC}/\mu_{IBC})^{1/3}$ ) and their depth at the time of LMO solidification using a Stokes' settling formulation [2,9] (Figs. 2b,2c).

**Results and implications:** The viscosity contrast between the IBC and mafic cumulates and the LMO solidification rate (~IBC sedimentation rate) determine the steady-state thickness of the IBC layer. Here we test two cases, a “dry” Moon with a viscosity contrast of  $2 \times 10^{-5}$  (red lines, Fig. 2) and a “wet” Moon with a viscosity contrast of  $7 \times 10^{-4}$  (blue lines). In the dry case the IBC layer is >10km thick for all reasonable LMO solidification rates (Fig. 2a) and would produce near-hemispheric instabilities at fast solidification rates (Fig. 2b). These would sink into the deep lunar mantle forming mare basalt source regions. An IBC diapir with hemispheric wavelength could explain the dichotomy of lunar basalt distributions on the surface [3].

In the wet case the IBC layer is thinner (Fig. 2a). Fast solidification produces IBC instabilities at hundreds of km wavelength that sink to the core-mantle boundary over the timescale of LMO solidification (Fig 2c). Slower solidification rates favor a thinner IBC layer and smaller instabilities. The wet case with a 200Myr solidification timescale recovers the scenario envisioned by [2], where small-scale IBC instabilities sink ~200km during LMO solidification producing a mixed IBC-mafic cumulate layer. Recent sample studies suggest a “wet” Moon with Earth-like water content and a hundreds-of-Myr LMO solidification timescale. These conditions favor the latter scenario, where sinking of small-scale IBC instabilities produces a mixed IBC-mafic cumulate

layer ~hundreds of km thick. Ongoing experimental work will constrain the rheology of this thicker mixed IBC-mafic cumulate layer. Future analysis will evaluate the importance of the assumption of constant stress, which likely exaggerates viscosity contrast compared to assumption of constant viscous dissipation rate, and radiogenic heat production in the IBC layer, which could significantly affect its viscosity, density, and solidification timescale.

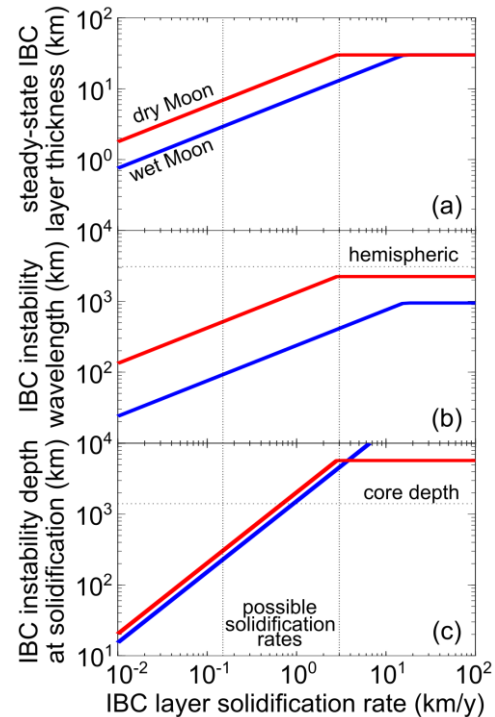


**Figure 2.** (a) Steady-state IBC layer thickness, (b) IBC instability wavelength, (c) IBC instability depth when LMO is fully solidified. Red and blue models correspond to wet and dry conditions (viscosity contrasts of  $7 \times 10^{-4}$  and  $2 \times 10^{-5}$ ).

**References:** [1] Ringwood, A., Kesson, S. (1976) *Proc. 7<sup>th</sup> LPSC*, 1697-1722. [2] Hess P., Parmentier, E. (1995) *EPSL*, 134, 501-514. [3] Parmentier, E., Zhong, S., Zuber, M. (2002) *EPSL*, 201, 473-480. [4] Dygert, N., Hirth, G., Liang, Y. (2015) *GRL*, 43, 532-540. [5] Tople, L. et al. (2017). *48<sup>th</sup> LPSC*, #1964. [6] Elkins-Tanton, L., Burgess, S., Yin, Q. (2011) *EPSL*, 304, 326-336. [7] Dygert, N. et al. (2017) *GRL*, 44(22), 11282-11291. [8] Boukaré, C., Parmentier, E., Parman, S. (2018) *EPSL*, 491, 216-225. [9] Whitehead, J. (1988) *Ann. Rev. F. Mech.* 20, 61-87. [10] Lin, Y., et al. (2017) *Nat. Geo.*, 10, 14-18. [11] Rapp, J., Draper, D. (2018) *Met. & P. Sci.*, 1-24. [12] Charlier, B., et al. (2018) *GCA*, 234, 50-96. [13] Zhao, Y., Zimmerman, M., Kohlstedt, D. (2018) *PEPI*, 278, 26-33. [14] Hirth, G., Kohlstedt, D. (2003), *Geophys. Mon.*, 138. [15] Zhang et al. (2017) *GRL*, 44, 6543-6552. [16] Wyatt, B., (1977) *CMP*, 61, 1-9. [17] Walker, D., et al. (1978), *GSA Bulletin*, 87, 646-656.